Supplementary Information

On-Surface Synthesis of Doubly-linked Porphyrin Polymers via Cycloaromatization of Isopropyl Substituents on Au(111)

Shenwei Chen[1, §], Haiwei Wang[1, §], Lixia Kang[2], Ran Chen[3], Zhaokun Wang[4], Suya Dai[1], Xiang Zhang[1], Yongjie Chen[1], Zhe Huang[1], Yucheng Song[1], Cunfeng Zheng[1], Zechao Yang[2], Zengfu Ou[5, *], Jin Li[1, *], Hongbing Ji[1, *]

[1] *State Key Laboratory of Green Chemical Synthesis and Conversion, College of Chemical Engineering, Zhejiang University of Technology, Hangzhou, Zhejiang, CN 310014*

[2] *School of Physics, Hangzhou Normal University, Hangzhou, Zhejiang, CN 311121*

[3] *Centre of the Protection and Monitoring for Cultural Heritage, Yungang Academy, Datong, Shanxi, CN 037007*

[4] *School of Chemistry and Chemical Engineering, Guangxi University, Nanning, Guangxi, CN 530004*

[5] *College of Physics and Electronic Information Engineering, Guilin University of Technology, Guilin, Guangxi, CN 541004*

[§] *S. C. and H. W. contributed equally to this work.*

Corresponding authors: Z. O. ouzengfu@glut.edu.cn; J. L. lijin@zjut.edu.cn; H. J. jihb@zjut.edu.cn

Methods

Sample preparation and STM experiments

All the STM and STS experiments were performed at 78 K using a commercial Createc LT-STM system. The base pressure was better than 1.0×10^{-10} mbar. All annealing steps involved heating the sample to the specified temperature, holding it for 30 minutes, cooling it to room temperature (RT), and then imaging at 78 K. The tip used in the experiments was a tungsten tip, which was etched using a 3 mol/L NaOH solution. STM images were acquired in constant-current mode, and all scanning probe images were processed using WSxM software.[1] For the V_s and I_t: V_s is the voltage applied to the sample; I_t is the corresponding tunneling current. A typical set point of 100 pA was used for the dI/dV spectra. To improve the signal-to-noise ratio, the lock-in amplifier was used with a modulation amplitude of 100 mV, where 100 mV corresponds to peak-to-peak. An atomically clean Au(111) substrate (purchased from MaTecK GmbH) was prepared through repeated cycles of argon ion (Ar+) bombardment (0.8 kV for 20 min) and annealing (750 K for 20 min). The 5,10,15,20-Tetrakis[4-(1-methylethyl) phenyl]-21H,23H-porphine (TIPP) was synthesized following the reported procedure[2] and thermally sublimated onto the Au(111) surface at approximately 590 K under a vacuum of ~3×10^{-9} mbar using a commercial molecular evaporator.

DFT Calculations

Density functional theory (DFT) calculations were performed using the Vienna Ab Initio Simulation Package.[3, 4] The projector augmented wave method was employed to treat the core electrons.[5] The Perdew-Burke-Ernzerhof functional based on generalized gradient approximation was used to describe the exchange–correlation interactions.[6, 7] All calculations were performed on freestanding atomic structures (without substrates). The plane-wave cutoff energy was set to 500 eV, and a vacuum layer of 15 Å was applied along the z direction to avoid interlayer interactions. The structures were fully relaxed until the residual forces on each atom were below 1×10^{-2} eV/Å and the total energy converged within 10^{-5} eV, with all atoms constrained to remain in the same plane by fixing their z coordinates. For the optimized structures of both pristine and Au-metalated DPPs (Fig. 4), the lattice periodicity along the molecular backbone was determined to be 19.2 Å, whereas for the hypothetical structure lacking the bridging phenyl units (Fig. S11), the optimized lattice periodicity was reduced to 14.9 Å. The results of the DFT calculations were visualized using VASPKIT and Pymatgen.[8]

Additional images

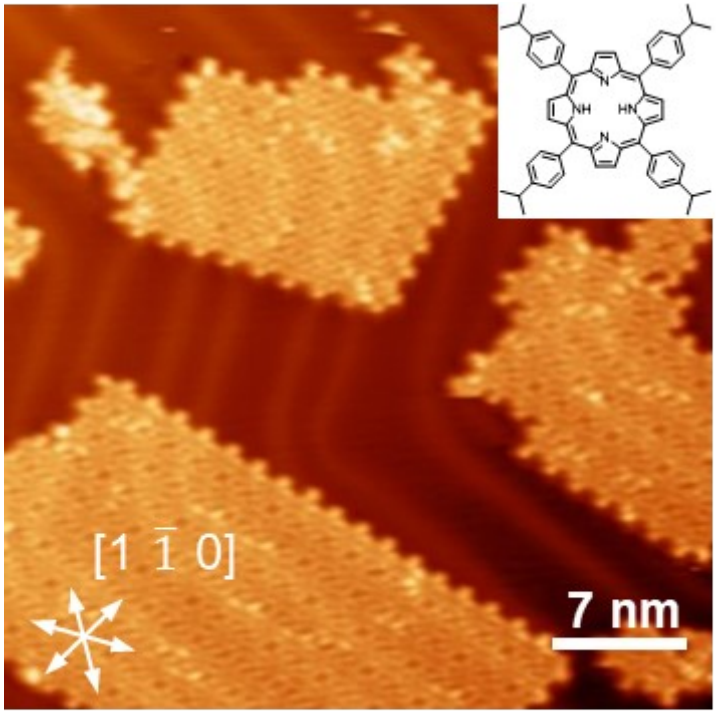

Figure S1 Large-scale STM image of self-assembled structure of TIPP molecules after deposition on the Au(111) surface held at RT. Tunneling parameters: $V_s = -2.0$ V, $I_t = 200$ pA.

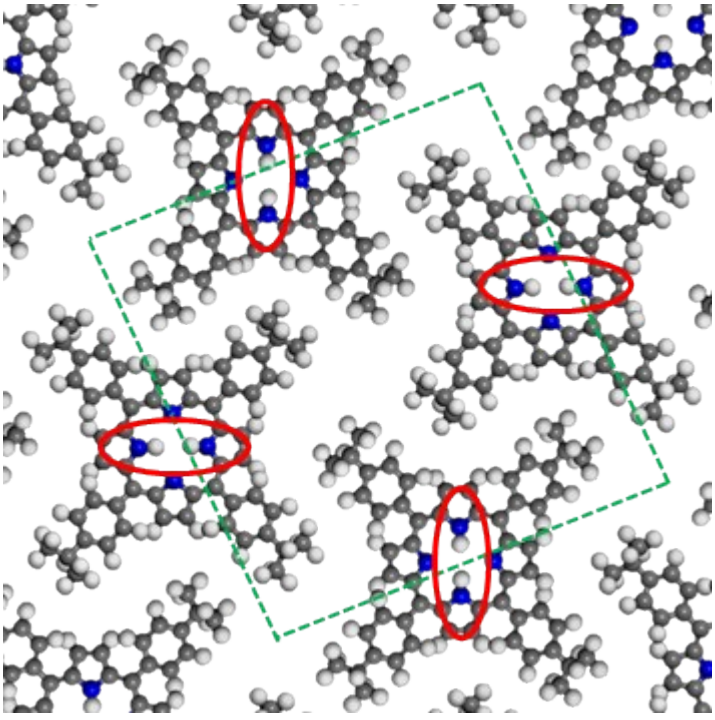

Figure S2 Schematic model of self-assembly of TIPP molecules, adjacent molecules have rotated 90 degrees between each other.

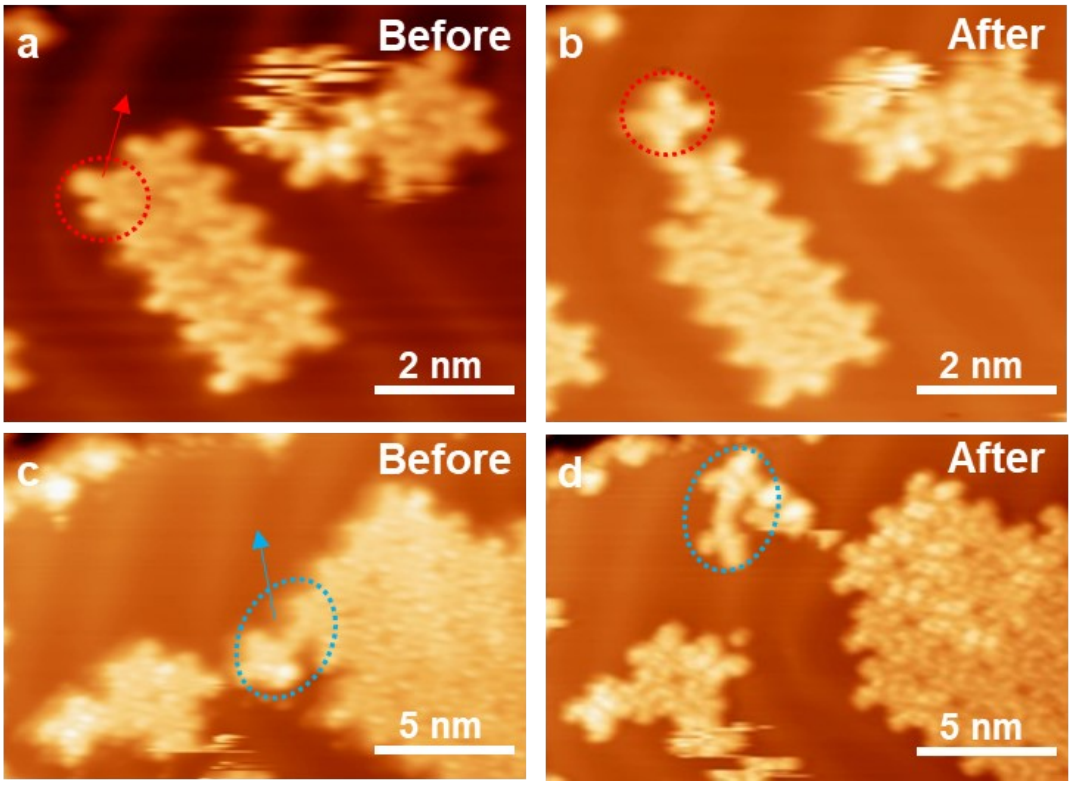

Figure S3 The sequential operation STM images of the tip manipulation. (a) and (b) STM images before and after the tip manipulation. The molecular model in (b) indicates that the force between molecules are non-covalent bonds. (c) and (d) STM images before and after the tip manipulation. The molecular model in (d) indicates that covalent bond formed between molecules. The arrows represent the direction of movement. Tunneling parameters: (a-d) $V_s = -1.0$ V, $I_t = 100$ pA.

The tip manipulation experiments were conducted in accordance with the method reported in the literature,[9, 10] which comprises four steps: (1) make the STM tip approaching the target molecule with high tunnel current (≈ 1 nA); (2) pick-up the molecule and retracting the STM tip with low bias (≈ − 50 mV); (3) lateral movement of the tip (together with the molecule); (4) release of the molecule by a voltage pulse of − 2.0 V, leaving the molecule adsorbed on the Au(111) surface.

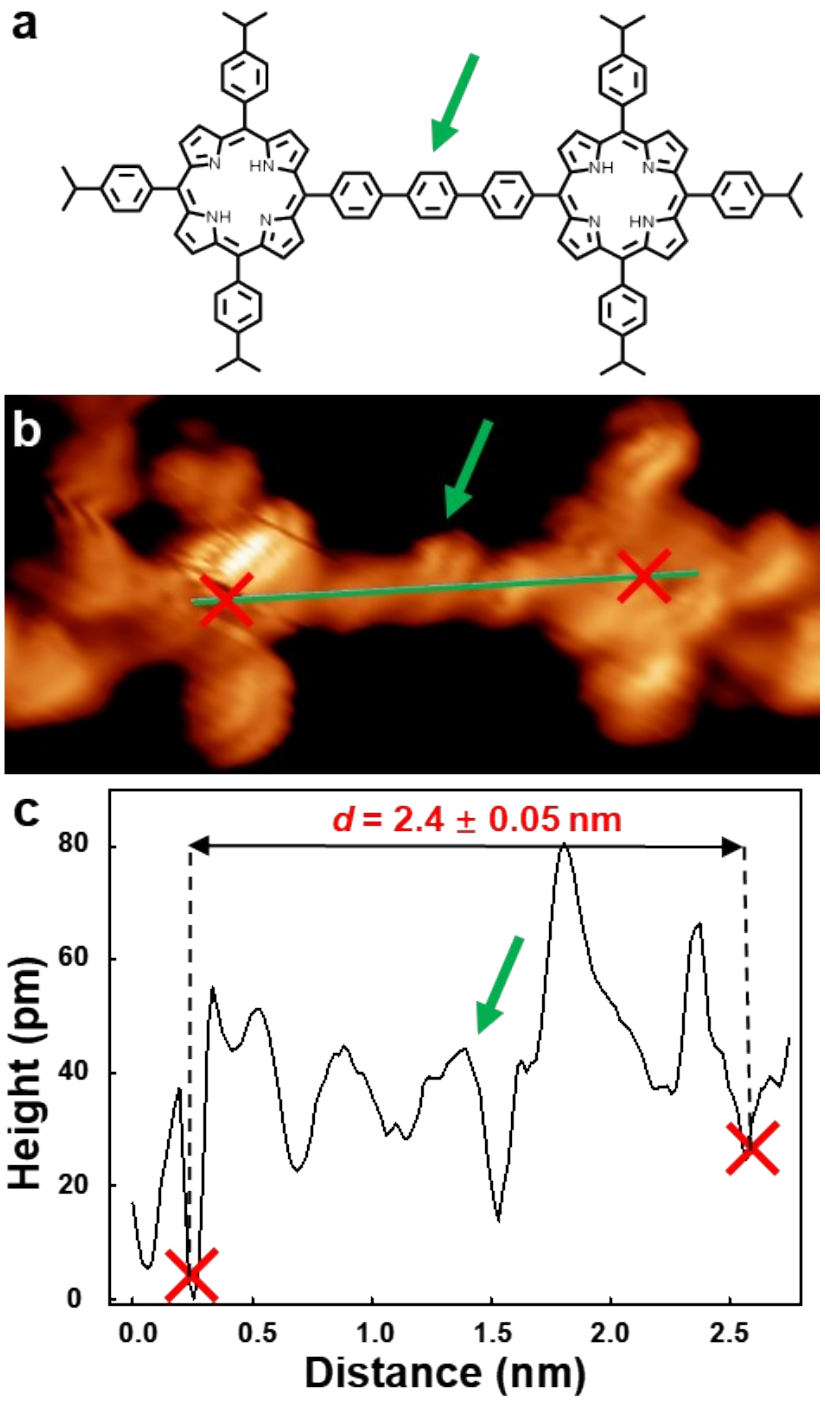

Figure S4 (a-c) Chemical structure, close-up STM image and profile elevation map of the structure **3**, a six-membered ring formed by [3+3] cycloaromatization. Tunneling parameters: V_s = − 1.0 V, I_t = 100 pA.

The distance between two TIPP molecules is measured to be **2.4 ± 0.05 nm**. A conspicuous protrusion in the profile elevation map (indicated by the green arrow) corresponds to the six-membered ring formed by [3+3] cycloaromatization, which is in excellent agreement with the chemical structure and corresponding STM image as illustrated in Fig. S4a and S4b.

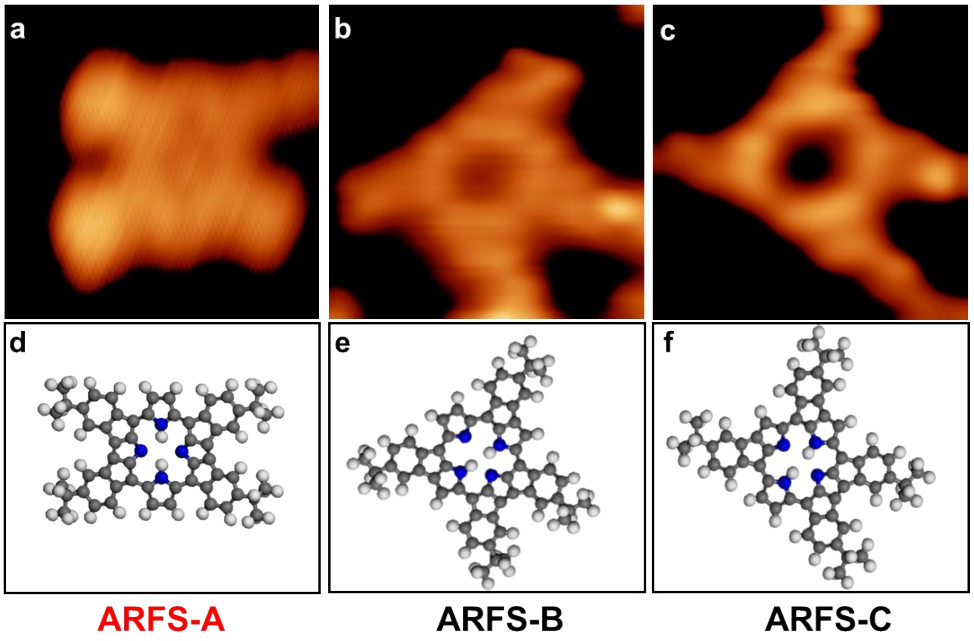

Figure S5 STM images (a-c) and simulated-structures (d-f) of three distinct **ARFSs**. Tunneling parameters: (a) $V_s = -1.5$ V, $I_t = 200$ pA. (b, c) $V_s = 1.0$ V, $I_t = 270$ pA.

Upon annealing the sample to approximately 450 K, the four meso-position substituents on the TIPP molecules engage in cyclodehydrogenation with the central porphyrin core, adopting various orientations. This process results in the creation of three unique types of aromatic ring-fused structures (**ARFSs**), which we have designated as **ARFS-A**, **ARFS-B**, and **ARFS-C**, respectively. Among which the **ARFS-A** is the predominant configuration. This is contributed to the favorable formation energy of the ARFS-A compared to the other two forms.[11]

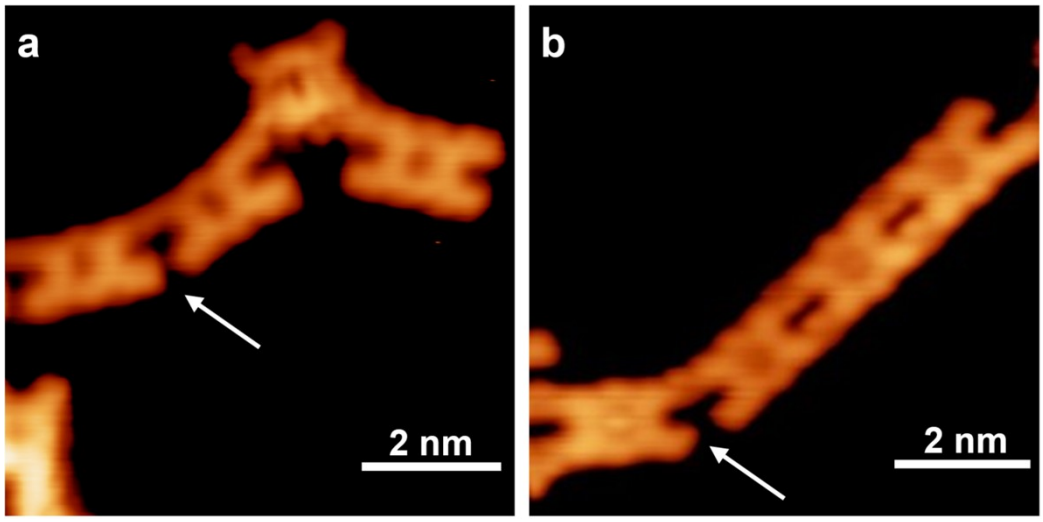

Figure S6 (a) and (b) STM images of intermediate **4** (marked by white arrows) after annealing the sample at 450 K. Tunneling parameters: (a) $V_s = 1.0$ V, $I_t = 100$ pA; (b) $V_s = -1.5$ V, $I_t = 170$ pA.

Figure S7 STM image of the DPPs with 5 units. Tunneling parameters: $V_s = -1.0$ V, $I_t = 120$ pA.

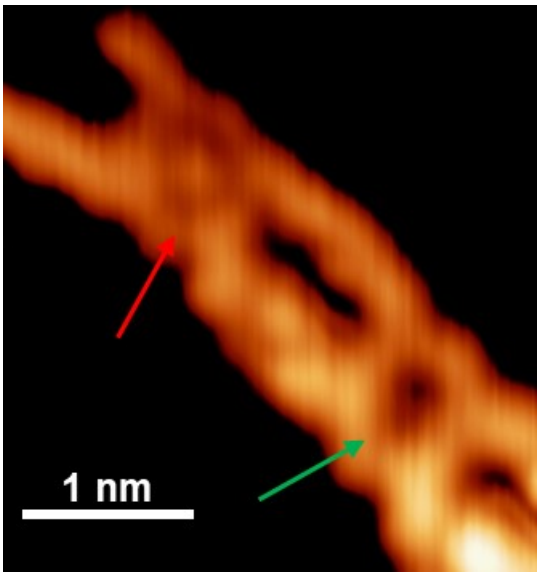

Figure S8 STM image of the DPPs with (red arrow) and without (green arrow) Au adatoms involved in coordination. Tunneling parameters: $V_s = 0.5$ V, $I_t = 300$ pA.

With the annealing temperature elevated, Au adatoms participate in the coordination with TIPP molecules. Fig. S8 shows the comparison between the coordination with Au adatoms and without Au adatoms after annealed at 450 K.

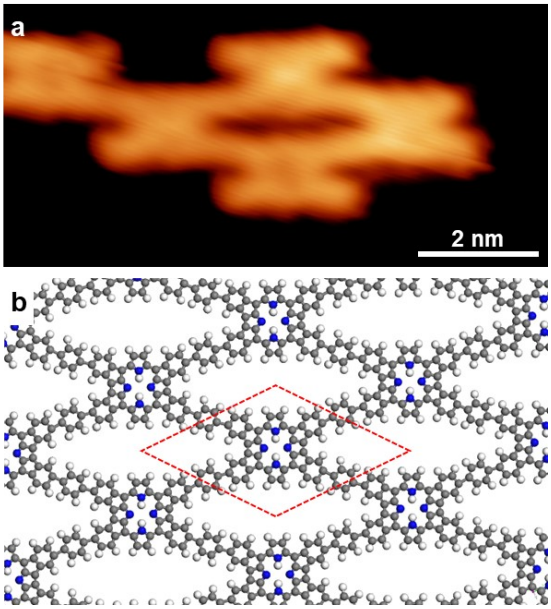

Figure S9 (a) STM image and (b) corresponding structural model of the 2D structure formed by [3+3] cycloaromatization. Tunneling parameters: $V_s = -0.6$ V, $I_t = 350$ pA.

We also observed the 2D structure that formed by TIPP molecules through [3+3] cycloaromatization. However, the area of this structure was relatively small and could not be extended over a large area. This limitation is likely due to steric hindrance.

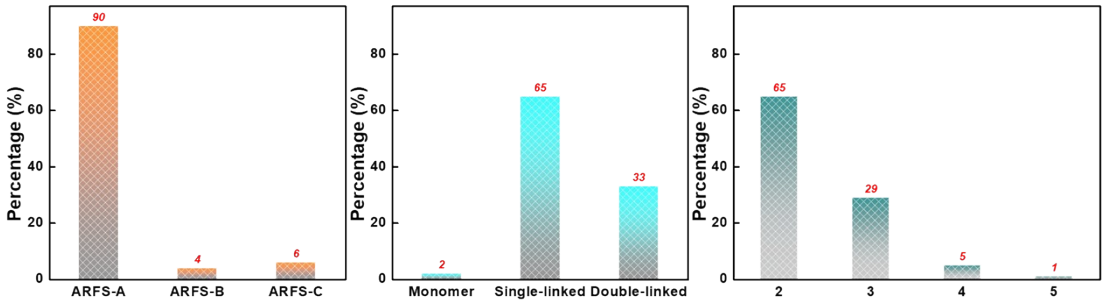

Figure S10 (a) Selectivity statistics for the intramolecular cyclization of TIPP. (b) Statistical analysis of the two connection modes (single linked or double linked). (c) Statistical analysis of the lengths of the doubly-linked porphyrin polymers.

Firstly, it is worth noted that the selective source of the target product arises from two aspects: the selective intramolecular cyclization of TIPP and the connection mode between ARFS-A monomers (whether it is single linked or double linked). Based on statistical samples of more than 2,000 molecules, the following conclusion can be drawn:

(1) For the selective intramolecular cyclization of TIPP. The selective intramolecular cyclization of TIPP is attributed to the different orientations with the cyclodehydrogenation. This phenomenon is attributed to the favorable formation energy and has been reported in literatures. Based on this, we conducted a detailed statistical analysis of the selectivity of the serval configurations in this work and obtained the following table. The ARFS-A is the predominant configuration with a selectivity of 90% as shown in Fig. S10a.

(2) For the connection mode between TIPP monomers, we conducted a statistical analysis of those two connection modes (single linked or double linked), Single linked refers to the connection mode between two molecules as shown in Fig. S6 or S9. The result revealed that the selectivity is 65% and 33%, respectively. In addition, a small number of monomers (2%) were also discovered as indicated in Fig. S10b.

(3) We further analyzed the lengths of the doubly-linked porphyrin polymers and reached the following conclusions as shown in Fig. S10c.

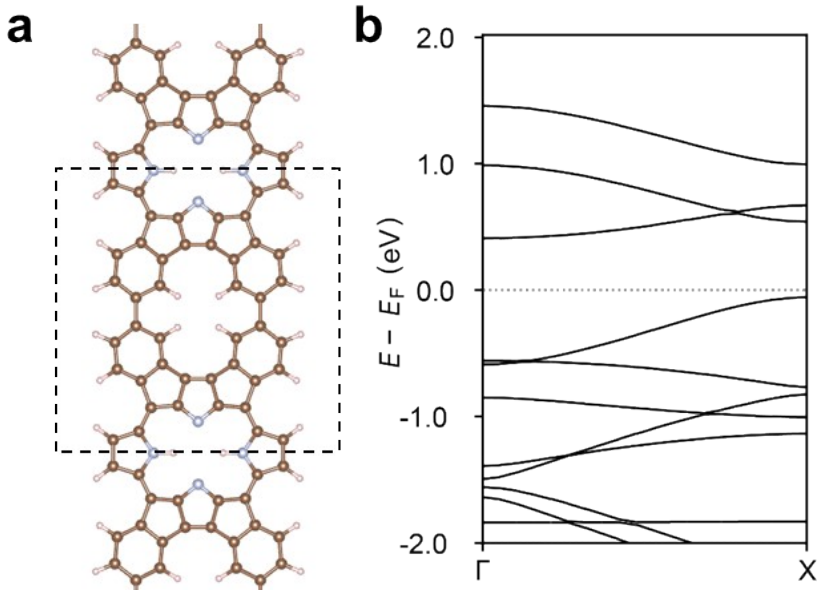

Figure S11 DFT-calculated results of a hypothetical structure lacking the bridging phenyl rings: (a) optimized structural model; (b) calculated band structure.

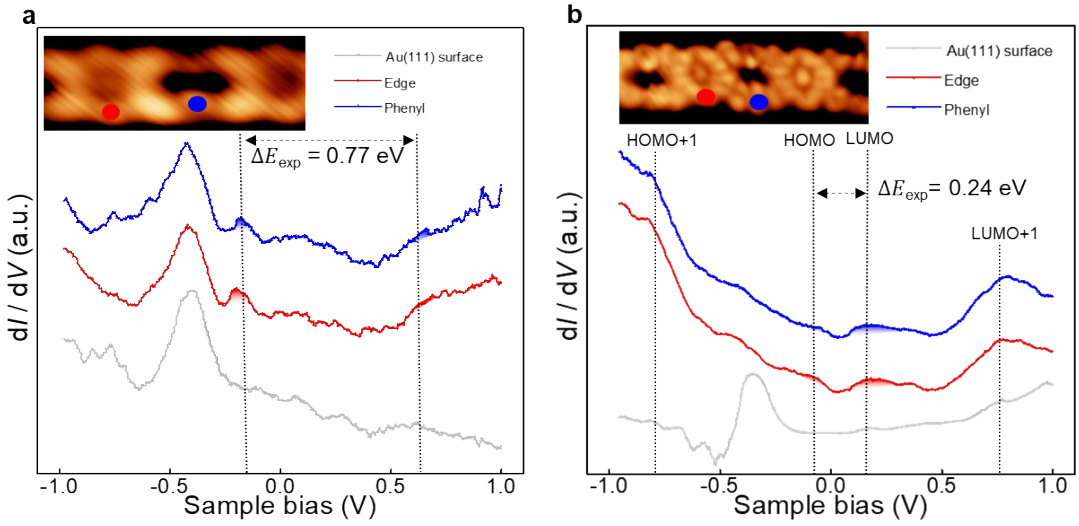

Figure S12 (a) dI/dV point spectra acquired at representative positions (marked by colored circles in the inset) of pristine DPPs. (b) dI/dV point spectra acquired at representative positions (marked by colored circles in the inset) of Au-metallized DPPs. Tunneling parameters: (a) V_s = − 1.0 V, I_t = 100 pA, (b) V_s = − 1.0 V, I_t = 450 pA.

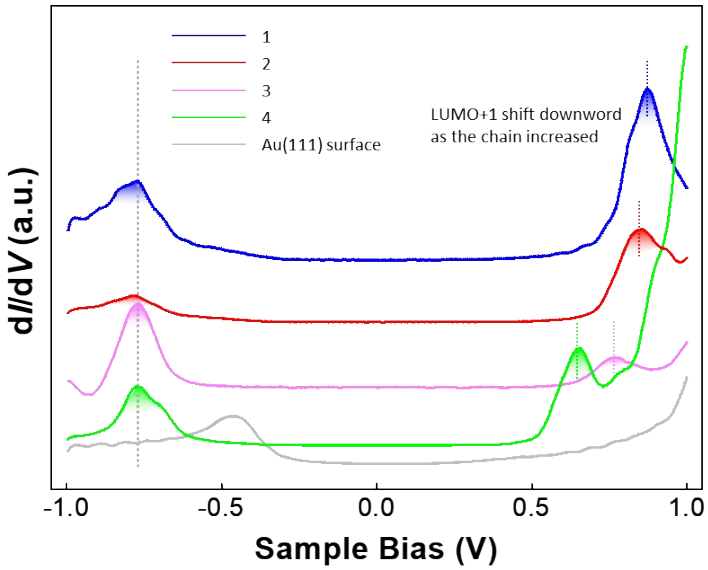

Figure S13 d*I*/d*V* spectra of Au-metallized DPPs with different lengths.

References

1 I. Horcas, R. Fernández, J. M. Gómez-Rodríguez, J. Colchero, J. Gómez-Herrero, et al., *Rev. Sci. Instrum.,* 2007, **78**, 013705.

2 L. Zamani and B. B. F. Mirjalili, *Chem. Heterocycl. Compd. (N. Y., NY, U. S.),* 2015, **51**, 578-581.

3 G. Kresse and J. Furthmüller, *Comput. Mater. Sci.,* 1996, **6**, 15-50.

4 G. Kresse and J. Furthmüller, *Phys. Rev. B,* 1996, **54**, 11169-11186.

5 P. E. Blöchl, *Phys. Rev. B,* 1994, **50**, 17953-17979.

6 J. P. Perdew, K. Burke and M. Ernzerhof, *Phys. Rev. Lett.,* 1996, **77**, 3865-3868.

7 J. P. Perdew, A. Ruzsinszky, G. I. Csonka, O. A. Vydrov, G. E. Scuseria, et al., *Phys. Rev. Lett.,* 2008, **100**, 136406.

8 G. Henkelman, A. Arnaldsson and H. Jónsson, *Comput. Mater. Sci.,* 2006, **36**, 354-360.

9 S. Wang, L. Talirz, C. A. Pignedoli, X. Feng, K. Müllen, et al., *Nat. Commun.,* 2016, **7**, 11507.

10 B. Yang, K. Niu, F. Haag, N. Cao, J. Zhang, et al., *Angew. Chem. Int. Ed.,* 2022, **61**, e202113590.

11 Y. Chen, W. Yi, P. Ding, Y. Sun, L. Kantorovich, et al., *Nano Lett.,* 2024, **24**, 12522-12528.